AJNR

Distinguishing Recurrent Intra-Axial Metastatic Tumor from Radiation Necrosis Following Gamma Knife Radiosurgery Using Dynamic Susceptibility-Weighted Contrast-Enhanced Perfusion MR Imaging

R.F. Barajas, J.S. Chang, P.K. Sneed, M.R. Segal, M.W. McDermott and S. Cha

AJNR Am J Neuroradiol published online 20 November 2008
http://www.ajnr.org/content/early/2008/11/20/ajnr.A1362.citation

Published November 20, 2008 as 10.3174/ajnr.A1362

Distinguishing Recurrent Intra-Axial Metastatic Tumor from Radiation Necrosis Following Gamma Knife Radiosurgery Using Dynamic Susceptibility-Weighted Contrast-Enhanced Perfusion MR Imaging

ORIGINAL RESEARCH

R.F. Barajas
J.S. Chang
P.K. Sneed
M.R. Segal
M.W. McDermott
S. Cha

BACKGROUND AND PURPOSE: MR image–guided gamma knife radiosurgery is often used to treat intra-axial metastatic neoplasms. Following treatment, it is often difficult to determine whether a progressively enhancing lesion is due to metastatic tumor recurrence or radiation necrosis. The purpose of our study was to determine whether relative cerebral blood volume (rCBV), relative peak height (rPH), and percentage of signal-intensity recovery (PSR) derived from dynamic susceptibility-weighted contrast-enhanced perfusion MR imaging can distinguish recurrent metastatic tumor from radiation necrosis.

MATERIALS AND METHODS: Twenty-seven patients with systemic cancer underwent gamma knife radiosurgery for metastatic lesions of the brain and subsequently developed enlarging regions of enhancement within the radiation field. Subsequent surgical resection or clinicoradiologic follow-up established a diagnosis of recurrent metastatic tumor or radiation necrosis. Perfusion MR imaging datasets were retrospectively reprocessed, and regions of interest were drawn around the entire contrast-enhancing region. The resulting T2* signal-intensity time curves produced rCBV, rPH, and PSR values for each examination. A Welch *t* test was used to compare imaging values between groups.

RESULTS: The mean, minimum, and maximum PSR values were significantly lower ($P < .01$) in cases of recurrent metastatic tumor. The mean and maximum rCBV and rPH values were significantly higher ($P < .02$) in the recurrent metastatic tumor group.

CONCLUSIONS: The findings of our study suggest that perfusion MR imaging may be used to differentiate recurrent intra-axial metastatic tumor from gamma knife–induced radiation necrosis.

BRAIN

ORIGINAL RESEARCH

MR image–guided gamma knife radiosurgery is often used to treat intra-axial metastatic neoplasms.[1] This conformal radiosurgery technique precisely delivers a single finely focused high dose of radiation to well-defined small intracranial targets, killing tumor cells within the irradiated target area; however, delayed radiation necrosis can occur, manifesting as progressive contrast enhancement on follow-up serial imaging. Metastatic tumor recurrence and radiation necrosis often have a similar appearance on conventional contrast-enhanced MR imaging.[2,3] As a result, it is often difficult to distinguish which entity is responsible for the appearance of a progressively enhancing lesion. A patient's clinical course, biopsy, and serial imaging for several months have traditionally been used to distinguish tumor recurrence and radiation necrosis.[1-3]

Newer MR imaging techniques have significantly advanced beyond the sole use of anatomic imaging. For example, physiologic MR imaging methods, such as dynamic susceptibility-weighted contrast-enhanced (DSC) perfusion MR imaging, have made it possible to obtain hemodynamic measurements within the brain.[4-12] DSC perfusion MR imaging exploits the susceptibility effect of a gadolinium-based contrast agent within the intravascular compartment and allows the measurement of 3 hemodynamic imaging variables: relative cerebral blood volume (rCBV), relative peak height (rPH), and percentage of signal-intensity recovery (PSR). rCBV is the most widely used hemodynamic variable derived from DSC perfusion MR imaging and has been shown to correlate with primary glioma tumor grade and tumor microvascular density.[4-12] rPH, which represents the maximal change in signal intensity during the passage of contrast agent, has been shown to correlate with rCBV measurements and tumor capillary blood volume.[5,6,12] Finally, PSR, an indicator of blood-brain-barrier integrity, reflects the degree of contrast agent leakage through tumor microvasculature and provides insight into the alteration of capillary permeability.[5,6,12]

Elevated microvascular density and elevated capillary permeability are pathologic features that distinguish metastatic tumor from irradiated brain tissue.[13-18] The ability to quantify a tumor's hemodynamic properties has shown promise for distinguishing malignant glial neoplasms from single brain

Received July 10, 2008; accepted after revision September 16.

From the Departments of Radiology (R.F.B., J.S.C., S.C.), Neuroradiology Section; Oncology (P.K.S.); Epidemiology and Biostatistics (M.R.S.); and Neurological Surgery (M.W.M., S.C.); University of California, San Francisco, San Francisco, Calif.

This work was supported by NS045013 and TL1 RR024129-01 from the National Center for Research Resources, a component of the National Institutes of Health (NIH) and NIH Roadmap for Medical Research.

Paper previously presented at: Annual Meeting of the American Society of Neuroradiology, May 31–June 5, 2008; New Orleans, La.

Please address correspondence to: Soonmee Cha, MD, UCSF Department of Radiology, 505 Parnassus Ave, Long L200B, Box 0628, San Francisco, CA 94143; e-mail: soonmee.cha@radiology.ucsf.edu

Indicates article with supplemental on-line table.

DOI 10.3174/ajnr.A1362

metastasis[5]; however, it remains unknown whether DSC hemodynamic measurements can add additional information that helps distinguish gamma knife–induced radiation necrosis from recurrent metastatic tumor in patients who present with progressive contrast enhancement on follow-up post-gamma knife serial imaging. Therefore, the purpose of our study was to determine whether rCBV, rPH, and PSR derived from DSC perfusion MR imaging can distinguish recurrent intra-axial metastatic tumor from gamma knife–induced radiation necrosis.

Materials and Methods

Patient Population

Of 517 patients treated with gamma knife radiosurgery at the University of California, San Francisco, from March 2002 to March 2007, 33 were selected for this retrospective study on the basis of the following criteria: diagnosis of primary systemic cancer, brain MR imaging consistent with metastatic intra-axial tumor, treatment with stereotactic gamma knife radiosurgery, subsequent progressively enlarging regions of contrast enhancement based on ≥2 consecutive MR images within the radiation field suggestive of tumor recurrence or radiation necrosis, MR imaging with a DSC perfusion sequence performed to evaluate the enlarging lesion, and surgical resection or adequate clinicoradiologic follow-up time to definitively determine diagnosis.

The presence of blood products or melanin within metastatic lesions, particularly those of melanoma and lung histologic origin, can cause a significant degree of susceptibility artifacts, making DSC perfusion measurements difficult. Six patients with melanoma brain metastases were excluded from this study due to high levels of susceptibility artifacts. No other patients in our study had lesions with a significant hemorrhagic component that disrupted DSC perfusion measurements.

All patients underwent follow-up MR imaging in intervals of ≤3 months once the post-gamma knife progressively enhancing regions were observed. None of the patients received additional radiation therapy to the brain during this follow-up period. All patients continued therapeutic treatment of the primary tumor when clinically indicated. Final determination between recurrent metastatic tumor and gamma knife–induced radiation necrosis for the enlarging progressively enhancing lesion was made either histologically or clinicoradiologically. Patients with >1% viable tumor on biopsy were classified as having a recurrence for the purposes of this study.

For lesions that were not histologically confirmed, radiation necrosis was diagnosed when progressively enhancing areas decreased definitively in size or remained unchanged on serial follow-up MR imaging for a minimum of 3 months. The length of enhancement stability on follow-up imaging in patients clinically diagnosed with radiation necrosis ranged from 9 to 30 months. Recurrent metastatic tumor was clinically diagnosed when the enhancing lesion progressively increased in size on serial examinations, accompanied by neurologic deterioration during a minimum follow-up period of 3 months. The duration of progressive enhancement on follow-up imaging in patients clinically diagnosed with recurrent metastatic tumor ranged from 8 to 21 months.

Imaging Protocol

All MR images were obtained with a 1.5T MR imaging scanner (Signa Horizon; GE Healthcare, Milwaukee, Wis). Conventional anatomic and gadolinium-enhanced MR images were acquired at each imaging time point following the same MR imaging protocol: 3-plane localizer (TR/TE, 8.5/1.6 ms), axial fluid-attenuated inversion recovery (FLAIR; TR/TE/TI, 10,000/148/2200 ms), axial fast spin-echo T2-weighted (TR/TE, 3000/102 ms), DSC gradient-echo echo-planar (TR/TE, 1000–1250/54 ms; flip angle, 35°), and contrast-enhanced 3D spoiled gradient-recalled (SPGR) T1-weighted (TR/TE, 34/8 ms) images. SPGR sequences were obtained with a 5-mm section thickness and a 1-mm intersection gap.

FLAIR and fast spin-echo images determined the location, size, and position of the lesion's superior and inferior margins for DSC gradient-echo echo-planar imaging. Seven to 8 sections (3–5 mm thick, gap of 1 mm) were used to cover the entire lesion volume. A standard dose of contrast agent, gadopentetate dimeglumine (Gd-DTPA; 0.1 mmol/kg of body weight; Omniscan, GE Healthcare), was injected intravenously with an MR imaging–compatible power injector (Spectris Solaris; Medrad, Indianola, Pa) at a rate of 4 or 5 mL/s through an antecubital angiocatheter (18–21 gauge), followed immediately by a 20-mL continuous saline flush. The multisection image set was obtained every 1.25 seconds during the first pass of the contrast agent until 60 time points were obtained.

Image Processing

The postcontrast 3D SPGR and raw DSC gradient echo-planar images were transferred to a commercially available perfusion image processing workstation (Advantage Workstation, GE Healthcare). Image processing was performed in a blinded manner by using commercially available software (FuncTool, GE Healthcare). The contrast-enhanced 3D SPGR images were registered to the same section locations and resolution as those of the echo-planar perfusion images.

Cerebral blood volume (CBV) maps and corresponding T2* susceptibility signal-intensity–time curves were derived on a voxel-by-voxel basis from the DSC imaging sets. An example of the resampled postcontrast SPGR image, T2*-derived CBV map, and corresponding T2* susceptibility signal-intensity time curves is shown in Fig 1. For each transaxial plane, regions of interest were drawn around the entire contrast-enhancing region (ECER) from the resampled contrast-enhanced 3D SPGR image. In addition, a measurement was gathered, in which a 50-mm^2 region of interest was drawn around the enhancing region with highest CBV and another 50-mm^2 region of interest was drawn around the contralateral normal-appearing white matter (NAWM) in the same transaxial plane to standardize the imaging data for normal between-patient hemodynamic variability. Regions of signal intensity dropout caused by susceptibility artifacts on the echo-planar images were excluded from the regions of interest because the T2* signal-intensity time curves within these voxels did not pass a certain signal-intensity-to-noise threshold to reliably quantify. All regions of interest were approved by a blinded attending neuroradiologist certified by the American Board of Radiology with a Certificate of Added Qualification in neuroradiology.

T2 Signal-Intensity Time Curve Analysis Derived from DSC Perfusion MR Imaging*

The resampled T2* signal-intensity time curves generated for each region of interest were used in the quantification of rCBV, rPH, and PSR (Fig 1).

The peak height (PH) and PSR were calculated as illustrated in Fig 1. rCBV was calculated as the ratio of the CBV within the enhancing region to the CBV within contralateral NAWM. PH values for each region of interest were determined by calculating the difference between the baseline precontrast signal intensity (S_o) and the lowest

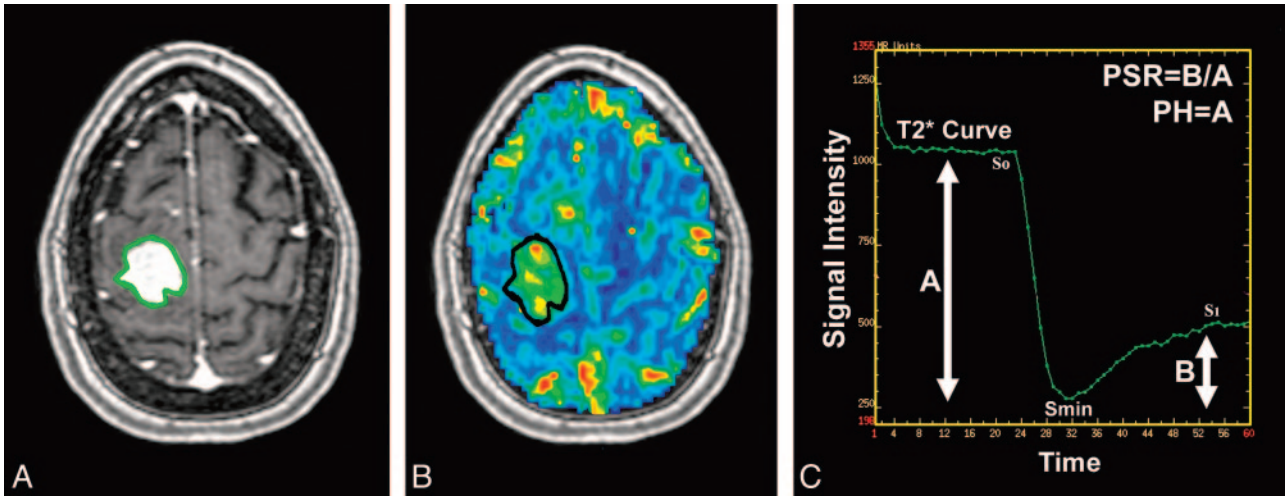

Fig 1. Perfusion examination No. 7. A 54-year-old woman with a history of recurrent metastatic non-small cell lung cancer 7.7 months after gamma knife radiosurgery. *A* and *B*, Contrast-enhanced SPGR T1-weighted image (*A*) and CBV map (*B*) with a single region of interest surrounding the entire contrast-enhancing region demonstrate an enhancing region with corresponding elevated CBV within the right posterior frontal and parietal lobes. *C*, Representative T2* signal-intensity time curve obtained from a single region of interest demonstrates PH represented as A ($S_o - S_{min}$) and PSR calculated as B / A ($S_1 - S_{min}/S_o - S_{min}$).

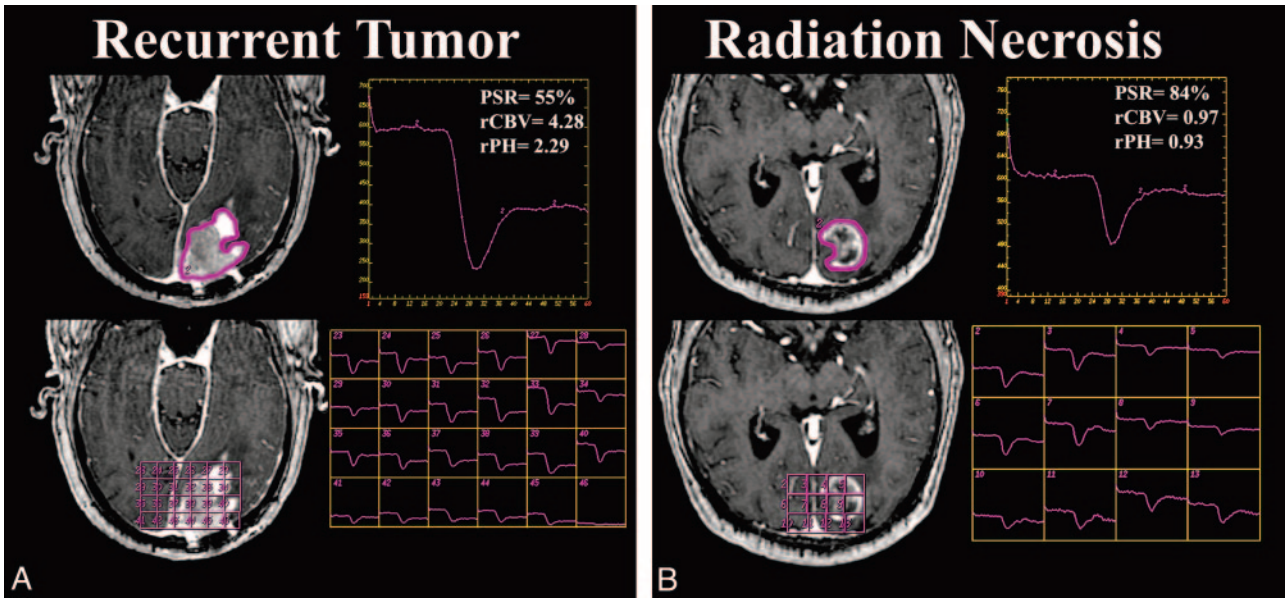

Fig 2. Transverse contrast-enhanced SPGR T1-weighted images (left) and T2* relaxivity-derived signal-intensity time curves (right) in histologically proved recurrent metastatic intra-axial adenocarcinoma of the lung (*A*) and radiation necrosis (*B*) show a significant difference in rCBV, rPH, and PSR. *A*, Perfusion MR imaging No. 16. Left occipital enhancing lesion in a 69-year-old man 17.9 months after metastatic tumor resection and gamma knife radiosurgery. A single region of interest surrounding the enhancing region (top) and a region of interest overlying the NAWM and enhancing region (bottom) demonstrate markedly elevated rCBV and rPH associated with 55% PSR. *B*, Perfusion MR imaging No. 31. A 66-year-old man with a left occipital enhancing lesion histologically proved to be due to radiation necrosis 4.3 months after gamma knife radiosurgery. A single region of interest surrounding the enhancing region (top) and a region of interest overlying NAWM and the enhancing region (bottom) demonstrate slightly decreased rCBV and rPH associated with 84% PSR. Considerable heterogeneity in the shape of the dynamic concentration time curves is noted throughout the contrast-enhancing lesion in both patients.

signal intensity (S_{min}) during passage of the contrast bolus. The value derived from this calculation was then normalized to the PH of the contralateral NAWM through a proportion of ratios, resulting in rPH. PSR was determined by calculating the percentage of the signal-intensity recovery from the lowest signal intensity of the contrast bolus (S_{min}) to the end postcontrast signal intensity−intensity (S_1). Mean, maximum, and minimum rCBV, rPH, and PSR were calculated from the contrast-enhanced region for each transaxial section in every case. The average of the mean, maximum, and minimum for perfusion variables for all transaxial sections was calculated for each patient.

Figure 2 demonstrates an example of various T2* relaxivity signal-intensity time curve characteristics in NAWM, recurrent intra-axial metastatic disease, and progressive enhancement caused by radiation necrosis on a T1 postcontrast image.

Statistical Analysis

Univariate analyses comparing mean, minimum, and maximum rCBV, rPH, and PSR imaging values between recurrent metastatic tumor and radiation necrosis groups were conducted by using a 2-sample Welch *t* test. This test generalizes the conventional *t* test by not prescribing that between-group variances are equal. A *P* value $< .05$ was considered to indicate a statistically significant difference between the hemodynamic measurements of the 2 groups. Thresh-

Table 1: Gamma knife treatment parameters and elapsed time to imaging and diagnosis*

Final Diagnosis	GK Target Volume (mL)	IDL (mL)	IDL (%)	GK Dose (Gy)	Time to MRI (days)†	Time to Final Diagnosis (days)‡	Imaging Follow-Up Time (days)§
Recurrent tumor	6.38 (5.2)	8.14 (6.5)	52 (0.7)	16.85 (1.1)	307 (149)	432 (327)	462 (195)
Radiation necrosis	4.29 (3.7)	5.46 (4.1)	54 (0.1)	17.55 (0.8)	301 (118)	353 (171)	402 (237)
Welch *P* value	.22	.18	.61	.06	.89	.40	.86

Note:—IDL indicates isodose line.
*All data are presented in mean values (SD).
†Represents number of days elapsed between initial radiosurgery and perfusion MR imaging examination.
‡Represents number of days elapsed between initial radiosurgery and final determination of metastatic tumor recurrence or radiation necrosis.
§Represents number of days elapsed between time of clinical diagnosis and loss to follow-up or death.

Table 2: PSR, rCBV, and rPH imaging values*

Final Diagnosis	Mean PSR	Max PSR	Min PSR	Mean rCBV	Max rCBV	Min rCBV	Mean rPH	Max rPH	Min rPH
Recurrent tumor	60.64 (9.95)	69.65 (9.52)	51.98 (12.76)	2.38 (0.95)	3.46 (2.19)	1.42 (0.65)	1.58 (0.55)	1.65 (1.32)	1.59 (1.88)
Radiation necrosis	83.33 (3.59)	86.96 (4.50)	79.25 (6.98)	1.54 (0.92)	2.04 (1.29)	0.95 (0.70)	1.03 (0.49)	1.1 (1.03)	0.9 (0.94)
Welch *P* value	<.01	<.01	<.01	.024	<.01	.079	<.01	<.01	<.01
95% CI RT	(56.6, 64.7)	(65.8, 73.5)	(46.8, 57.2)	(2.00, 2.76)	(2.57, 4.35)	(1.16, 1.68)	(1.36, 1.80)	(1.12, 2.19)	(0.82, 2.36)
95% CI RN	(81.2, 85.5)	(84.3, 89.6)	(75.1, 83.4)	(0.99, 2.08)	(1.28, 2.80)	(0.54, 1.36)	(0.75, 1.31)	(0.49, 1.71)	(0.35, 1.45)

Note:—95% CI indicates 95% confidence interval; RT, recurrent tumor; max, maximum; min, minimum.
*All data are presented in mean values (SD).

olds for dichotomizing the individual markers were obtained by using classification trees,[19] with attendant predictive performance assessed via cross-validation. Analyses were conducted by using the *R* statistical package.[20]

Results

Patient Population

Twenty-seven patients (16 women and 11 men) with previously diagnosed systemic cancer (14 with adenocarcinoma of the lung, 1 with squamous cell carcinoma of the lung, 1 with non-small cell carcinoma of the lung, 8 with breast adenocarcinoma, 2 with renal cell cancer, and 1 with extremity sarcoma) underwent DSC perfusion MR imaging to monitor progressively enhancing lesions previously treated with gamma knife radiosurgery.

Three of the 27 patients had 2 independent lesions for a total of 30 lesions evaluated. Twenty lesions were diagnosed as recurrent brain metastases (18 histologically). Ten lesions were diagnosed as resulting from radiation necrosis without the presence of viable metastatic tumor (4 histologically).

Four of the 30 lesions were evaluated on 2 separate occasions because of a second episode of progression for a total of 34 perfusion MR imaging examinations. Of the 34 MR imaging examinations, 23 showed lesions representing recurrent tumor and 11 showed lesions representing radiation necrosis. Patient and lesion characteristics are provided in on-line Table 1.

One patient was lost to follow-up 14.0 months after radiosurgery, 8 were alive 15.7–68.7 months (mean, 35.7 months) after radiosurgery, and 18 patients died 7.2–47.2 months (mean, 22.2 months) after radiosurgery. Diagnosis and survival data are provided in on-line Table 1.

Contrast-Enhancing Volumes, Radiation Dosage, and Time to Final Diagnosis

On-line Table 1 summarizes the findings of 34 DSC perfusion MR imaging examinations included in this study. Considerable heterogeneity was noted in the shape of the dynamic concentration time curves in both the recurrent tumor and radiation necrosis groups (Fig 2).

Table 3: Sensitivity and specificity for the detection of radiation necrosis using PSR, rCBV, and rPH values*

Statistic	PSR COV = 76.3	rCBV COV = 1.54	rPH COV = 0.69
Sensitivity	95.65	91.30	86.96
Specificity	100.00	72.73	45.45

Note:—COV indicates cutoff value.
*All data are presented as percentages.

Contrast-enhancing lesions that later recurred tended to have larger target volumes and lower prescribed doses at the time of gamma knife radiosurgery compared with lesions later found to have resulted from radiation necrosis ($P > .05$) (Table 1). The difference in elapsed time between initial radiosurgery and the onset of lesion enlargement was not found to be statistically significant between the 2 groups (Table 1).

The mean volume of enhancing regions on DSC perfusion T1-weighted postcontrast images was found to be higher in subjects with recurrent tumor (mean, 3.27 mL; SD, 3.7 mL) than in those with lesions resulting from radiation necrosis (mean, 2.14 mL; SD, 2.2 mL), but this difference was not statistically significant ($P = .29$). There was no significant difference in time to perfusion MR imaging examination (range, 73–748 days), time to final diagnosis (range, 75–1578 days), or imaging follow-up time (range, 247–931 days) between the 2 groups (Table 1).

Percentage of Signal Intensity Recovery

Compared with the radiation necrosis group, subjects with recurrence of metastatic tumor had statistically significant lower mean, minimum, and maximum PSR values within contrast-enhancing regions ($P < .01$) (Table 2). PSR values >76.3% were indicative of radiation necrosis, in that a cutoff value of 76.3% yielded a sensitivity of 95.65% and a specificity of 100% (Table 3).

rCBV and rPH

Mean and maximum rCBV and rPH values from the entire enhancing region were significantly higher within the recur-

rent metastatic tumor group than the radiation necrosis group (Table 2). An rPH cutoff value of 0.69 did not withstand cross-validation for differentiating recurrent tumor and radiation necrosis ($P > .05$). However, a cutoff rCBV value of 1.52 did withstand cross-validation and yielded a sensitivity of 91.30% and a specificity of 72.73% (Table 3). rCBV values < 1.35 were only observed in enhancing regions, consistent with radiation necrosis ($n = 6$). Figure 2 highlights an example of how DSC perfusion values varied between the recurrent metastatic tumor and radiation necrosis groups. The level of statistical significance for quantified T2* signal-intensity time intensity data was unchanged when comparing the region of interest placed around the ECER with the region of interest around the 50-mm^2 area of highest CBV.

Discussion

In this study using DSC perfusion MR imaging, we found that PSR, an imaging indicator of microvascular leakiness, was the most significant variable able to distinguish retrospectively whether a progressively enhancing lesion was due to recurrent metastatic tumor or gamma knife–induced radiation necrosis.

Microvascular leakage, measured by DSC perfusion MR imaging, provides important insight into tumor biology. Several histology-based studies have demonstrated that the degree of capillary permeability varies markedly between recurrent intra-axial metastatic tumor and radiosurgery-induced necrosis. Long,[15] in the electron microscopy examination of tumor capillary ultrastructure, showed that capillaries of metastatic intra-axial tumors resemble those of their systemic origin rather than capillaries of native brain tissue. Kamiryo et al[14] have demonstrated that the blood-brain-barrier architecture of capillaries within previously irradiated brain tissue remains relatively intact, whereas metastatic tumor capillaries are inherently leaky. Metastatic tumor capillaries are highly permeable to macromolecular contrast agents because they lack blood-brain-barrier architecture, which is unique to native brain capillaries.[5,15-18]

Our findings of significantly lower PSR values in the recurrent tumor group are consistent with what has previously been described histopathologically. Capillary permeability measured by DSC perfusion MR imaging within enhancing regions of recurrent metastatic intra-axial tumors is much higher than that of enhancing regions due to radiation necrosis. This finding is very likely because metastatic tumor capillaries lack the blood-brain barrier that would limit contrast leakiness. The measurement of PSR resulted in the most significant difference between the 2 groups studied. There was little overlap between the PSR values resulting from these groups, suggesting that PSR may be a better prognostic indicator of metastatic tumor recurrence than rCBV or rPH.

In this study, mean and maximum rCBV and rPH imaging variables were also found to be significantly higher in the recurrent metastatic tumor group than in the radiation necrosis group. This result is consistent with existing literature,[5,12] which has suggested that DSC perfusion may be used to distinguish single brain metastasis and malignant glial neoplasms due to the markedly increased expression of microvascular density by high-grade gliomas.

In the present study, a large degree of overlap of rCBV and rPH values was observed between the recurrent metastatic tumor and radiation necrosis groups. This overlap may have been due to a number of factors, including anatomic tumor heterogeneity and the inability of DSC measurements to distinguish the elevated microvascular density of recurrent metastatic tumor from hyperplastic dilated vasculature changes that occur within radiation necrosis.

Regions of enhancement caused by recurrent metastatic tumor were noted to be highly heterogeneous. In our study, histologic analysis of enhancing tissue from the recurrent metastatic tumor group revealed >50% tissue necrosis in most of the tissue samples. This tumor heterogeneity very likely accounts for some of the observed overlap of rCBV and rPH values.

Several other imaging techniques are currently used in clinical practice in an attempt to differentiate recurrent tumor from radiation necrosis. The use of fluorodeoxyglucose–positron-emission tomography (PET) to distinguish these 2 entities has been studied with mixed results. Some institutions report high accuracy,[21-23] whereas others report that PET is neither sensitive nor specific enough to be used routinely.[24,25] Coregistration of anatomic MR images with physiologic images of PET has been proposed as a way to improve the accuracy of PET.

Proton MR spectroscopy has also been used to differentiate recurrent tumor and radiation necrosis, with success. Previous studies have demonstrated the value of evaluating metabolic change in intra-axial neoplasms following radiation therapy by using proton MR spectroscopy to determine recurrent tumor,[26] and several studies have shown the utility of proton MR spectroscopy in differentiating recurrent tumor and radiation necrosis following radiation therapy of the brain.[27-29] However, these studies have primarily focused on recurrent gliomas versus radiation necrosis, and the few studies using MR spectroscopy to differentiate specifically metastatic tumor recurrence and radiation necrosis have been relatively small.

To our knowledge, there has been no study that examines the use of DSC perfusion-derived PSR, rPH, and rCBV values to differentiate metastatic tumor recurrence and radiation necrosis in patients with progressively enhancing lesions following gamma knife radiosurgery. However, because the number of patients in our study was small and only 4 patients were histologically diagnosed with radiation necrosis, we would caution against overinterpretation of our study results. In the future, a more systematic evaluation with a greater sample size and direct image-guided histopathologic investigation of hemodynamic characteristics of recurrent metastatic tumor and radiation necrosis should be undertaken. Such a study may confirm the efficacy of the techniques described in this article.

Beyond our small sample size, our study had several limitations. Partial volume averaging within the regions of interest could have affected the data obtained from T2* relaxivity signal intensity time curves. Although we attempted to control for this averaging by obtaining a second standardized 50-mm^2 region of interest of an enhancing region with the highest CBV, the results between values obtained did not vary from the results of the unstandardized data.

Finally, a significant degree of susceptibility artifacts due to pooling blood products, melanin deposition, or extravasation of contrast material within intra-axial lesions was noted in 6

cases, preventing the investigation of metastatic melanoma. Sensitivity to susceptibility artifacts is a known limitation of perfusion imaging, often resulting in image degradation making DSC measurements difficult to obtain. To eliminate this limitation, future prospective studies may use sensitivity-encoding echo-planar imaging (EPI) sequences, which have been shown to produce a significant reduction in magnetic susceptibility–induced artifacts compared with the standard EPI 8-channel coil acquisition at 3T.[30]

Conclusions

In this study, we chose 3 hemodynamic variables to describe the shape of the signal intensity time curve obtained from DSC perfusion MR imaging because we wished to provide robust easy-to-obtain imaging variables that could be used for the clinical interpretation of images without the need for timely sophisticated off-line software processing.

Although the relatively small sample size of this retrospective study cautions against overinterpretation, our results suggest that quantitative analysis of signal-intensity time curves obtained from DSC perfusion MR imaging provides additional insight into tumor biology that in a clinical setting may, once prospectively validated, increase the specificity of distinguishing metastatic tumor recurrence from radiation necrosis.

Acknowledgments

The first author thanks Bethany Carlson and Ilona Garner for their helpful comments regarding this manuscript.

References

1. Mintz A, Perry J, Spithoff K, et al. **Management of single brain metastasis: a practice guideline.** *Curr Oncol* 2007;14:131–43
2. Tsuruda JS, Kortman KE, Bradley WG, et al. **Radiation effects on cerebral white matter: MR evaluation.** *AJR Am J Roentgenol* 1987;149:165–71
3. Dooms GC, Hecht S, Brant-Zawadzki M, et al. **Brain radiation lesions: MR imaging.** *Radiology* 1986;158:149–55
4. Sugahara T, Korogi Y, Tomiguchi S, et al. **Posttherapeutic intraaxial brain tumor: the value of perfusion-sensitive contrast-enhanced MR imaging for differentiating tumor recurrence from nonneoplastic contrast-enhancing tissue**. *AJNR Am J Neuroradiol* 2000;21:901–09
5. Cha S, Lupo JM, Chen MH, et al. **Differentiation of glioblastoma multiforme and single brain metastasis by peak height and percentage of signal intensity recovery derived from dynamic susceptibility-weighted contrast-enhanced perfusion MR imaging**. *AJNR Am J Neuroradiol* 2007;28:1078–84
6. Lupo JM, Cha S, Chang SM, et al. **Dynamic susceptibility-weighted perfusion imaging of high-grade gliomas: characterization of spatial heterogeneity.** *AJNR Am J Neuroradiol* 2005;26:1446–54
7. Essig M, Waschkies M, Wenz F, et al. **Assessment of brain metastases with dynamic susceptibility-weighted contrast-enhanced MR imaging: initial results.** *Radiology* 2003;228:193–99
8. Sugahara T, Korogi Y, Kochi M, et al. **Correlation of MR imaging-determined cerebral blood volume maps with histologic and angiographic determination of vascularity of gliomas.** *AJR Am J Roentgenol* 1998;171:1479–86
9. Lev MH, Ozsunar Y, Henson JW, et al. **Glial tumor grading and outcome prediction using dynamic spin-echo MR susceptibility mapping compared with conventional contrast-enhanced MR: confounding effect of elevated rCBV of oligodendrogliomas.** *AJNR Am J Neuroradiol* 2004;25:214–21
10. Cha S, Lu S, Johnson G, et al. **Dynamic susceptibility contrast MR imaging: correlation of signal intensity changes with cerebral blood volume measurements.** *J Magn Reson Imaging* 2000;11:114–19
11. Aronen HJ, Gazit IE, Louis DN, et al. **Cerebral blood volume maps of gliomas: comparison with tumor grade and histologic findings.** *Radiology* 1994;191:41–51
12. Law M, Cha S, Knopp EA, et al. **High-grade gliomas and solitary metastases: differentiation by using perfusion and proton spectroscopic MR imaging.** *Radiology* 2002;222:715–21
13. Oh BC, Liu CY, Wang MY, et al. **Stereotactic radiosurgery: adjacent tissue injury and response after high-dose single fraction radiation. Part 1. Histology, imaging, and molecular events**. *Neurosurgery* 2007;60:31–45
14. Kamiryo T, Lopes MB, Kassell NF, et al. **Radiosurgery-induced microvascular alterations precede necrosis of the brain neuropil**. *Neurosurgery* 2001;49:409–15
15. Long DM. **Capillary ultrastructure in human metastatic brain tumors**. *J Neurosurg* 1979;51:53–58
16. Remler MP, Marcussen WH, Tiller-Borsich J. **The late effects of radiation on the blood brain barrier.** *Int J Radiat Oncol Biol Phys* 1986;12:1965–69
17. Jinnouchi T, Shibata S, Fukushima M, et al. **Ultrastructure of capillary permeability in human brain tumor. Part 6. Metastatic brain tumor with brain edema** [in Japanese]. *No Shinkei Geka* 1988;16(5 suppl):563–68
18. Spiegelmann R; Friedmann WA, Bova FJ, et al. **LINAC radiosurgery: an animal model.** *J Neurosurg* 1993;78:638–44
19. Breiman L, Friedman JH, Olshen RA, et al. *Classification and Regression Trees.* Belmont, Calif: Wadsworth; 1984
20. *The R Project for Statistical Computing.* Available at: http://www.R-project.org. Accessed February 2008
21. Chao S, Suh J, Raja S, et al. **The sensitivity and specificity of FDG PET in distinguishing recurrent brain tumor from radionecrosis in patients treated with stereotactic radiosurgery**. *Int J Cancer* 2001;96:191–97
22. Ericson K, Kihlström L, Mogard J, et al. **Positron emission tomography using 18F-fluorodeoxyglucose in patients with stereotactically irradiated brain metastases.** *Stereotact Funct Neurosurg* 1996;66(suppl 1):214–24
23. Petronas NJ, DiChiro G, Brooks RA, et al. **Work in progress: [18F] fluorodeoxyglucose and positron emission tomography in the evaluation of radiation necrosis of the brain.** *Radiology* 1982;144:885–89
24. Griffeth LK, Rich KM, Dehdashti F, et al. **Brain metastases from non-central nervous system tumors: evaluation with PET.** *Radiology* 1993;186:37–44
25. Kahn D, Follett KA, Bushnell DL, et al. **Diagnosis of recurrent brain tumor: value of 201Tl SPECT vs 18F-fluorodeoxyglucose PET.** *AJR Am J Roentgenol* 1994;163:1459–65
26. Graves E, Nelson S, Vigneron D, et al. **Serial proton MR spectroscopic imaging of recurrent malignant gliomas after gamma knife radiosurgery.** *AJNR Am J Neuroradiol* 2001;22:613–24
27. Schlemmer H, Bachert P, Herfarth K, et al. **Proton MR spectroscopic evaluation of suspicious brain lesions after stereotactic radiotherapy.** *AJNR Am J Neuroradiol* 2001;22:1316–24
28. Hein P, Eskey C, Dunn J, et al. **Diffusion-weighted imaging in the follow-up of treated high-grade gliomas: tumor recurrence versus radiation injury.** *AJNR Am J Neuroradiol* 2004;25:201–09
29. Hollingworth W, Medina L, Lenkinski R, et al. **A systematic literature review of magnetic resonance spectroscopy for the characterization of brain tumors.** *AJNR Am J Neuroradiol* 2006;27:1404–11
30. Lupo JM, Lee MC, Han ET, et al. **Feasibility of dynamic susceptibility contrast perfusion MR imaging at 3T using a standard quadrature head coil and eight-channel phased-array coil with and without SENSE reconstruction**. *J Magn Reson Imaging* 2006;24:520–29